

REPORT DOCUMENTATION PAGE			1 Form Approved OMB NO. 0704-0188	
<p>The public reporting burden for this collection of information is estimated to average 1 hour per response, including the time for reviewing instructions, searching existing data sources, gathering and maintaining the data needed, and completing and reviewing the collection of information. Send comments regarding this burden estimate or any other aspect of this collection of information, including suggestions for reducing this burden, to Washington Headquarters Services, Directorate for Information Operations and Reports, 1215 Jefferson Davis Highway, Suite 1204, Arlington VA, 22202-4302. Respondents should be aware that notwithstanding any other provision of law, no person shall be subject to any penalty for failing to comply with a collection of information if it does not display a currently valid OMB control number.</p> <p>PLEASE DO NOT RETURN YOUR FORM TO THE ABOVE ADDRESS.</p>				
1. REPORT DATE (DD-MM-YYYY)		2. REPORT TYPE New Reprint		3. DATES COVERED (From - To) -
4. TITLE AND SUBTITLE Minority Carrier Lifetime in Beryllium-Doped InAs/InAsSb Strained Layer Superlattices			5a. CONTRACT NUMBER W911NF-12-2-0057	
			5b. GRANT NUMBER	
			5c. PROGRAM ELEMENT NUMBER 611102	
6. AUTHORS Youxi Lin, Ding Wang, Dmitry Donetsky, Gregory Belenky, Harry Hier, Wendy L. Sarney, Stefan P. Svensson			5d. PROJECT NUMBER	
			5e. TASK NUMBER	
			5f. WORK UNIT NUMBER	
7. PERFORMING ORGANIZATION NAMES AND ADDRESSES Research Foundation of SUNY at Stony Brc W-5510 Melville Library West Sayville, NY 11796 -3362			8. PERFORMING ORGANIZATION REPORT NUMBER	
9. SPONSORING/MONITORING AGENCY NAME(S) AND ADDRESS (ES) U.S. Army Research Office P.O. Box 12211 Research Triangle Park, NC 27709-2211			10. SPONSOR/MONITOR'S ACRONYM(S) ARO	
			11. SPONSOR/MONITOR'S REPORT NUMBER(S) 62447-EL.14	
12. DISTRIBUTION AVAILABILITY STATEMENT Approved for public release; distribution is unlimited.				
13. SUPPLEMENTARY NOTES The views, opinions and/or findings contained in this report are those of the author(s) and should not contrued as an official Department of the Army position, policy or decision, unless so designated by other documentation.				
14. ABSTRACT Minority carrier lifetimes in undoped and Beryllium-doped Type-2 Ga-free, InAs/InAsSb strained layer superlattices (SLS) with energy gaps as low as 0.165 eV were determined from photoluminescence kinetics. The minority carrier lifetime of 450 ns at 77 K in the undoped SLS confirms a high material quality. In similarly-grown structures that were p-doped to $N_A = 6 \times 10^{16}$ and $3 \times 10^{17} \text{ cm}^{-3}$, electron lifetimes of $\tau_n = 45 \text{ ns}$ and 8 ns were measured. The $6 \times 10^{16} \text{ cm}^{-3}$ doping level is a factor of 6 greater than the typical background doping level in long wave infrared (LWIR) GaSb containing InAs/CaSb SLS with similar bandgap and electron lifetime. This				
15. SUBJECT TERMS MBESLSLWIR photodetectorInAs/InAsSbcarrier lifetime				
16. SECURITY CLASSIFICATION OF:			17. LIMITATION OF ABSTRACT UU	15. NUMBER OF PAGES
a. REPORT UU	b. ABSTRACT UU	c. THIS PAGE UU		
				19a. NAME OF RESPONSIBLE PERSON Gregory Belenky
				19b. TELEPHONE NUMBER 631-632-8397

Report Title

Minority Carrier Lifetime in Beryllium-Doped InAs/InAsSb Strained Layer Superlattices

ABSTRACT

Minority carrier lifetimes in undoped and Beryllium-doped Type-2 Ga-free, InAs/InAsSb strained layer superlattices (SLS) with energy gaps as low as 0.165 eV were determined from photoluminescence kinetics. The minority carrier lifetime of 450 ns at 77 K in the undoped SLS confirms a high material quality. In similarly-grown structures that were p-doped to $N_A = 6 \times 10^{16}$ and $3 \times 10^{17} \text{ cm}^{-3}$, electron lifetimes of $\tau_n = 45$ ns and 8 ns were measured. The $6 \times 10^{16} \text{ cm}^{-3}$ doping level is a factor of 6 greater than the typical background doping level in long-wave infrared (LWIR) Ga-containing InAs/GaSb SLS with similar bandgap and electron lifetime. This suggests that LWIR photodetectors with InAs/InAsSb SLS absorbers can be designed with smaller minority carrier concentrations and diffusion dark current densities. A relatively slow decrease of the lifetime with doping suggests a minor role of Auger recombination in the studied Ga-free SLS at $T = 77$ K with p-doping up to mid- 10^{17} cm^{-3} level.

REPORT DOCUMENTATION PAGE (SF298) (Continuation Sheet)

Continuation for Block 13

ARO Report Number 62447.14-EL
Minority Carrier Lifetime in Beryllium-Doped InA...

Block 13: Supplementary Note

© 2014 . Published in Journal of Electronic Materials, Vol. Ed. 0 43, (9) (2014), (, (9). DoD Components reserve a royalty-free, nonexclusive and irrevocable right to reproduce, publish, or otherwise use the work for Federal purposes, and to authorize others to do so (DODGARS §32.36). The views, opinions and/or findings contained in this report are those of the author(s) and should not be construed as an official Department of the Army position, policy or decision, unless so designated by other documentation.

Approved for public release; distribution is unlimited.

Minority Carrier Lifetime in Beryllium-Doped InAs/InAsSb Strained Layer Superlattices

Y. LIN,^{1,3} D. WANG,¹ D. DONETSKY,¹ G. BELENKY,¹ H. HIER,²
 W.L. SARNEY,² and S.P. SVENSSON²

1.—Stony Brook University, Stony Brook, NY 11794, USA. 2.—Army Research Laboratory, Adelphi, MD 20783, USA. 3.—e-mail: youxilin7@gmail.com

Minority carrier lifetimes in undoped and Beryllium-doped Type-2 Ga-free, InAs/InAsSb strained layer superlattices (SLS) with energy gaps as low as 0.165 eV were determined from photoluminescence kinetics. The minority carrier lifetime of 450 ns at 77 K in the undoped SLS confirms a high material quality. In similarly-grown structures that were *p*-doped to $N_A = 6 \times 10^{16}$ and $3 \times 10^{17} \text{ cm}^{-3}$, electron lifetimes of $\tau_n = 45$ ns and 8 ns were measured. The $6 \times 10^{16} \text{ cm}^{-3}$ doping level is a factor of 6 greater than the typical background doping level in long-wave infrared (LWIR) Ga-containing InAs/GaSb SLS with similar bandgap and electron lifetime. This suggests that LWIR photodetectors with InAs/InAsSb SLS absorbers can be designed with smaller minority carrier concentrations and diffusion dark current densities. A relatively slow decrease of the lifetime with doping suggests a minor role of Auger recombination in the studied Ga-free SLS at $T = 77$ K with *p*-doping up to mid- 10^{17} cm^{-3} level.

Key words: MBE, SLS, LWIR photodetector, InAs/InAsSb, carrier lifetime

INTRODUCTION

There is continued interest in the development of narrow-gap III–V semiconductor compound materials for the fabrication of mid-wave and long-wave infrared photodetectors. Type-2 InAs/GaSb strained layer superlattices (SLS) grown by molecular beam epitaxy (MBE) on GaSb substrates offer the important flexibility of energy band engineering and the possibility of Auger suppression.^{1,2} One can assume that absorber layers in Ga-containing type-II SLS structures are typically made *p*-type by Beryllium doping,^{3–5} and therefore that the photocurrent is dominated by electrons, since otherwise the impeded hole transport would limit the detector performance. In such structures, which had energy gaps corresponding to ~ 8 to $10 \mu\text{m}$ absorption and a typical background *p*-doping concentration of $1 \times 10^{16} \text{ cm}^{-3}$, electron lifetimes in the range of 30–45 ns at $T = 77$ K have been reported.^{6–8} As the deliberate doping concentration is increased, a rapid

reduction of the electron lifetime to 10 ns was observed for doping levels as low as $p\text{-}2 \times 10^{16} \text{ cm}^{-3}$.³ The limited carrier lifetime in the *p*-doped Type-2 InAs/GaSb SLS is commonly attributed to the Shockley–Read–Hall (SRH) carrier recombination through mid-gap energy centers located in the GaSb. Ga vacancies or Ga_{Sb} antisite centers could explain the short carrier lifetime.^{9,10} The observed rapid reduction of the carrier lifetime with Be doping beyond the $1 \times 10^{16} \text{ cm}^{-3}$ level points to the additional role of Be-related centers in carrier recombination. Due to the partial ionization of Be at liquid nitrogen temperatures,⁶ Be-derived neutral centers may capture minority electrons efficiently.⁷

Ga-free Type-2 InAs/InAsSb SLS grown on GaSb have been studied recently.^{11–19} The renewed interest in this material system is due to the observation of an order of magnitude greater minority carrier lifetime in undoped InAs/InAsSb SLS compared to that in InAs/GaSb SLS.^{17,18} Using this material system, a LWIR nBn photodetector was fabricated, with a detectivity $D^* \sim 10^{10} \text{ cmHz}^{1/2}/\text{W}$ and a quantum efficiency (QE) of 2.5% at 77 K with a 13.2- μm cut-off wavelength.²⁰ The modest QE was

(Received December 13, 2013; accepted May 3, 2014)

attributed to the impeded minority hole transport, which is in turn due to the wide InAs layers and therefore narrow hole mini bands. We suggest that, by changing the conductivity type from the natural n -type background doping to moderate p -doping, the photodetector QE should not be limited by minority carrier transport since the electron miniband, unlike the hole mini bands, is sufficiently wide. In other words, the origin of low QE in the nBn structure generally results from the low mobility of holes.

In this work, carrier recombination in InAs/InAsSb SLS, p -doped to $p = 6 \times 10^{16} \text{ cm}^{-3}$ and $p = 3 \times 10^{17} \text{ cm}^{-3}$, was studied. At $T = 77 \text{ K}$, minority carrier lifetime values of 45 ns and 8 ns, respectively, were measured. The product of the electron lifetime and background hole concentration at both doping levels was found to be nearly constant. This indicates the minor (if any) contribution of Auger recombination to the electron lifetime at 77 K in the studied InAsSb/InAs SLS with mid- 10^{17} cm^{-3} doping levels.

High QE values have been reported in the devices with InAs/GaSb SLS absorbers. At the same time, the minority carrier lifetime of 45 ns was reported for these materials.^{6,7} This demonstrates that the electron mobility in InAs/GaSb SLS is such that the 45-ns electron lifetime is sufficiently large and is not limiting QE. Assuming similar electron mobilities in InAs/InAsSb, equally high collection of the photo-carriers should be achieved in a Ga-free SLS.

HETEROSTRUCTURES FOR LIFETIME MEASUREMENTS

All SLS structures were grown in a Gen-II MBE system equipped with As and Sb crackers. The growth was performed at the substrate temperature of 490°C, measured with a K-space BandIT system operated in pyrometer mode. The growth rate was 1 $\mu\text{m/h}$. The InAsSb and InAs layers had the target thicknesses of 173 Å and 72 Å, respectively. The ratio of Sb/As beam equivalent pressures was in the range from 0.13 to 0.16. The InAsSb portions of the SLS period had Sb compositions that were varied in the range from 23.5% to 26.6% by adjusting beam equivalent pressures. The SLS region was 1 μm thick. The other characteristics of the samples are summarized in Table I.

The concentrations of free carriers in the p -doped SLS structures were confirmed by time-resolved

photoluminescence (TRPL) measurements. The layer thicknesses and Sb-mole fractions were determined from high-resolution x-ray diffraction data. Although the intent was to produce samples with the same bandgap, there were variations in the Sb-mole fraction that correlated approximately linearly with the PL wavelength, as seen in Table I. As and Sb beam equivalent pressure ratios were carefully set before the growths. However, data logging of the chamber background pressure, which is dominated by As, showed some unintended variations between growths, which correlated linearly with the resulting Sb-mole fraction.

EXPERIMENTAL SETUP

For spectral measurements, the photoluminescence (PL) was excited at 1064 nm by a Nd:YAG laser operating in the continuous-wave mode. The excitation area was 0.785 mm². The PL spectra were measured with a Nicolet Magna-860 Fourier transform infrared (FTIR) spectrometer, operating in either continuous-scan or step-scan mode with a 14- μm cut-off wavelength external HgCdTe photodetector. The PL kinetics were measured in both time and frequency domains. In the time domain, the lifetime was determined from PL decay after a short pulse excitation. In the frequency domain, the lifetime was determined from the bandwidth of PL response to a sine wave-modulated continuous-wave excitation. These approaches are referred to as time resolved PL (TRPL) and optical modulation response (OMR), respectively.

The TRPL measurements were conducted with excess carriers that were excited by a Q-switched Nd:YAG laser operating at 1064 nm with a repetition rate of 6 kHz and a pulse width of 0.7 ns. The OMR measurements were conducted with excess carriers that were excited with a fiber-coupled diode laser operating at 1.5 μm . In both approaches, the PL was collected by reflective optics and detected with a Vigo 10- μm cut-off, HgCdTe detector with a 3-ns time constant. The laser emission scattered from the sample surface was rejected with a 4.5- μm cut-off wavelength long-pass Ge filter. The sample temperature was stabilized with a closed-cycle He cryostat system from Janis with a M22 cryohead. A ZnSe window was used, which had a coating optimized for high transmission in the LWIR range. A description of the setup for OMR lifetime measurements can be found elsewhere.²¹

Table I. Summary of sample designs and resulting wavelengths and lifetimes

Sample	Barriers	p -doping	Sb-x	Lambda (micron)	Tau (ns)	Notation
K1048	No	No	0.235	6.5	450	U1
K1058	Yes	No	0.235	6.5	450	U2
K1225	Yes	6.E+16	0.266	7.7	45	P1
K1226	Yes	3.E+17	0.246	6.9	8	P2

PHOTOLUMINESCENCE SPECTRA

The PL spectra of the structures with undoped SLS regions measured at $T = 13$ K are shown in Fig. 1a. The excitation power was 100 mW, which resulted in a power density of 12.7 W/cm^2 . This was found to be adequate in previous experiments for determining the energy gap from low temperature PL maxima.¹⁹ The PL intensities were similar, in spite of the lack of AlSb confinement layers for U1. The PL peak energies correspond to a wavelength of $6.5 \mu\text{m}$ with a full-width at half-maximum of 14 meV, indicating high material quality. The undoped structures have n -type background doping and minority holes are well confined within the InAsSb portions of the SLS cell, which had sufficiently high barriers to impede hole transport. The slightly greater PL intensity for the structure without AlSb confinement layers could be due to different external quantum efficiencies since the carrier lifetimes were found to be identical.

The PL spectra for the Be-doped SLS structures are shown in Fig. 1b. The structures were measured with an excitation power of 60 mW. The excitation power density was 7.64 W/cm^2 . The PL maxima at $T = 13$ K were found to be at 7.7 and $6.9 \mu\text{m}$ for structures P1 (Sb composition of 26.3%) and P2 (Sb composition of 24.6%), respectively. The structure with higher Sb composition had a correspondingly longer PL peak wavelength. The FWHM of 11 meV for P1 and 14 meV for P2 are very similar to that for the undoped material shown in Fig. 1a. The PL intensity was stronger for the sample with the lower doping level, as expected. The ratio of PL intensities for P1 and P2 was about 5 times, consistent with the ratio of the background doping as expected at low excitation levels.

TRPL DATA AND DISCUSSION

The time-resolved PL decays are shown in Fig. 2 for all four samples measured at an excitation energy of 15 nJ. For U2, P1, and P2, the initial PL intensities, were similar. The PL intensity for U1 was stronger than that for U2, which correlates with spectral measurements shown in Fig. 1. All PL decays show a rapid response for several ns followed by longer decays, which can be fit by an exponential dependence with a time constant. The initial rapid response was attributed to the diffusion of excess carriers over the SLS region, followed by a longer period when the PL intensity is controlled by carrier recombination. The TRPL peak intensity (I_{PLmax}) taken at the beginning of the exponential recombination period was measured in a broad range of pulse excitation energies (Fig. 3). The dependence of I_{PLmax} versus the pulse excitation energy in double log scale showed an expected change of slope. The PL intensity, I_{PL} , is proportional to the product of the sum of the equilibrium and non-equilibrium hole concentrations ($p + \Delta p$) and the electron concentrations (Δn), $I_{\text{PL}} \propto (p + \Delta p) \Delta n$. The region at low excitation energies corresponds to a low

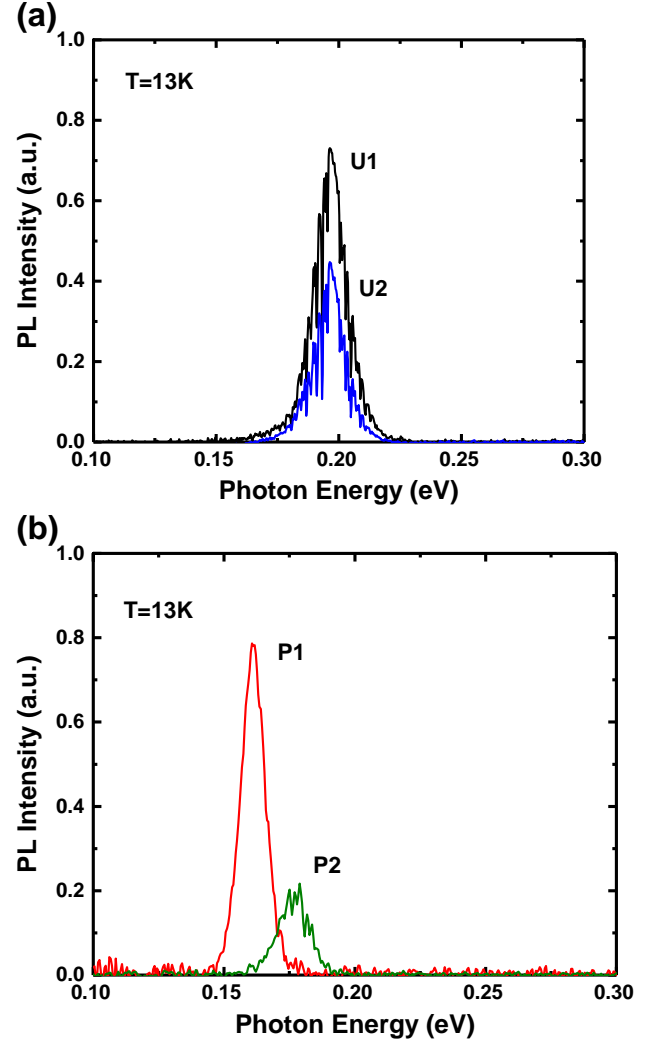


Fig. 1. The PL spectra of Ga-free SLS at 13 K. (a) Undoped samples with Sb compositions of 23.5% with AlSb cap (blue line), and without AlSb cap (black line). The excitation power was 100 mW. (b) p -doped samples with Sb = 24.6% (green line) and 26.3% (red line). The excitation power was 60 mW (Color figure online).

injection recombination mode where the concentration of excess electrons is small compared to the background hole concentration ($\Delta n \ll p$). The region with high excitation energies is attributed to a high injection ($\Delta n \gg p$) recombination mode. The transition region between the two recombination modes allowed us to verify the background hole concentration (p) determined from growth calibrations. After accounting for reflection from the sample surface, all photons were considered to be absorbed. The initial excess carrier concentration was calculated from the pulse energy divided by the volume of the excited SLS region. For p -doped samples, a homogenous distribution of excess electrons over the recombination region was assumed. The lines approximating low and high recombination modes intersect at $(8-9) \times 10^{16} \text{ cm}^{-3}$ for P1 and at $(2-3) \times 10^{17} \text{ cm}^{-3}$ for P2 which were fairly close to the design data.

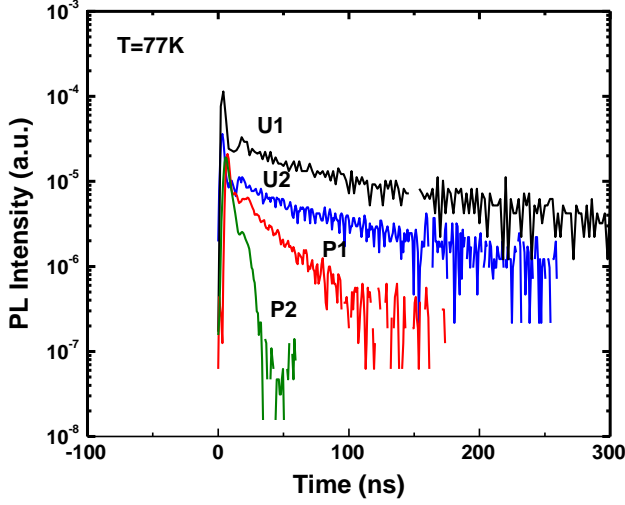


Fig. 2. The TRPL spectra of Ga-free SLS at 13 K. (a) Undoped samples with Sb compositions of 23.5% with AISb cap (blue line), and without AISb cap (black line). (b) *p*-doped samples with Sb = 24.6% (green line) and 26.3% (red line). The excitation energy per pulse was 15 nJ (Color figure online).

For the TRPL decays shown in Fig. 2, which were obtained with an excitation level of 15 nJ ($\lambda = 1064$ nm) per area of $8 \times 10^{-3} \text{ cm}^2$, the exponential fitting would result in PL decay time constants of 25 and 4.5 ns for structures P1 and P2, respectively. At this excitation level, the initial excess carrier concentration was estimated to be above $6 \times 10^{16} \text{ cm}^{-3}$. In general, the dependence of PL intensity on excess carrier concentration is non-linear, $I(PL) \propto (\Delta n)^k$. Using the TRPL approach, the minority carrier lifetime is obtained by multiplying the PL decay constant by the coefficient k . The accuracy of the determination of k limits the accuracy of carrier lifetime measurements by TRPL. A priori, the value of k is not known since the kinetics of carrier capture to recombination centers can be complicated. The value of coefficient k was difficult to extract because of excess noise at the lower end of excitation range. PL decay constants for excitation energies lower than 15 nJ were not determined because of the high noise level. While with long averaging the PL peak intensities were determined for excitation energies down to 4 nJ, the accuracy of measurements was decreasing with the decrease of excitation. A trend of increase of PL decay time constant with decreasing excitation was noticed. It is reasonable to expect the PL decay constant to continue to increase with further decrease of the excitation. The quantitative measurements of the minority carrier lifetime were performed by the OMR method, which allowed for the determination of the PL response time constants under significantly lower excess carrier concentrations. The reduction of noise was possible with significant reduction of the amplifier bandwidth from 50 MHz in TRPL method down to 1 Hz in the OMR method. The latter was realized with the use of a

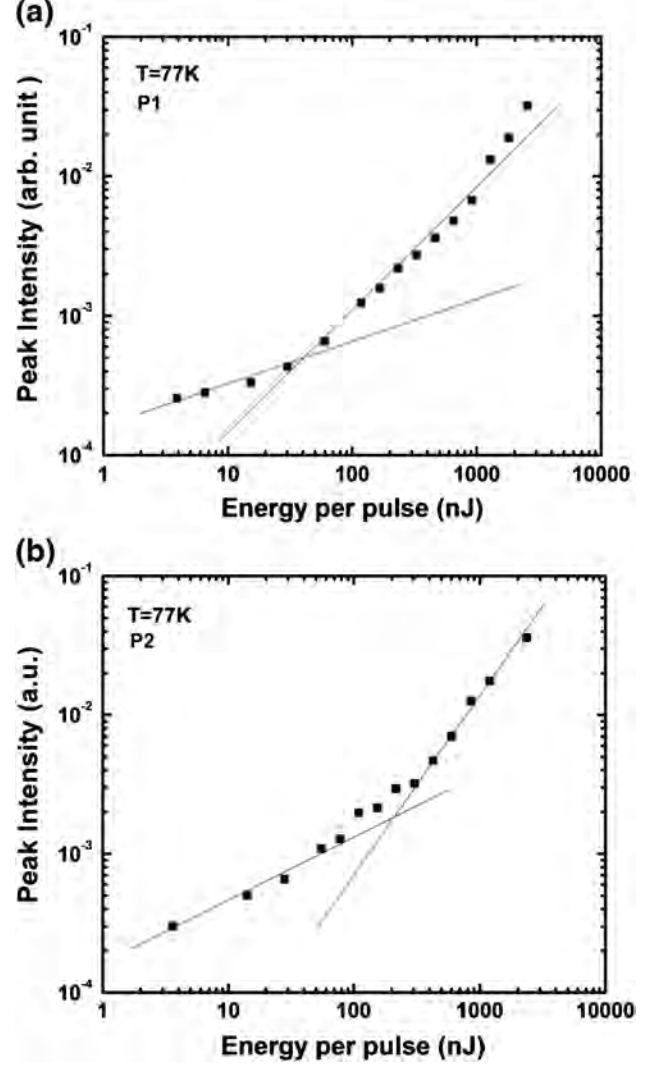


Fig. 3. The dependences of peak intensity from TRPL on the excess excitation carrier concentration at 77 K for (a) the $p = 6 \times 10^{16} \text{ cm}^{-3}$ structure, and (b) the $p = 3 \times 10^{17} \text{ cm}^{-3}$ structure.

lock-in-amplifier. In the OMR approach, the PL response signal is proportional to the first power of the excess carrier concentration since the harmonics are filtered out by the lock-in-amplifier.

OMR DATA AND DISCUSSION

The PL responses in the frequency domain measured for the four samples at the same carrier generation rate of $1.27 \times 10^{23} \text{ s}^{-1} \text{ cm}^3$ at $\lambda = 1.5 \mu\text{m}$ at power level 1.6 W/cm^2 are shown in Fig. 4a. The fitting in Fig. 4a with a response of a low-pass filter of first-order resulted in the carrier lifetime constants of 45 ns and 8 ns, for samples doped at $p = 6 \times 10^{16} \text{ cm}^{-3}$ and $p = 3 \times 10^{17} \text{ cm}^{-3}$, respectively. The excess carrier concentration at this excitation level was estimated to be $5.7 \times 10^{15} \text{ cm}^{-3}$, and $1 \times 10^{15} \text{ cm}^{-3}$ for P1 and P2, respectively. As shown in Fig. 4b, c, the PL bandwidth for P1 was found to be independent of excitation at lower

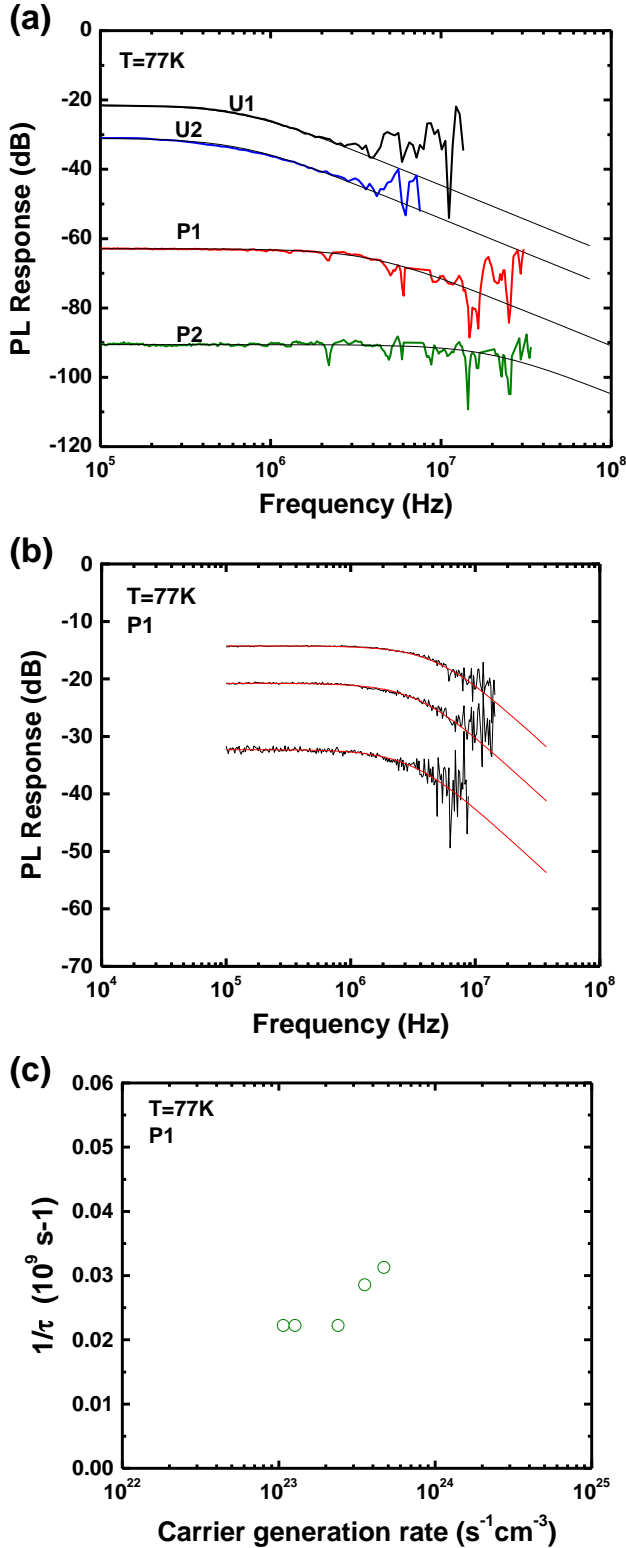


Fig. 4. The OMR of Ga-free SLS. (a) Undoped samples with Sb composition of 23.5% with AlSb barriers (blue line), without AlSb barriers (black line), and *p*-doped samples with 26.3% Sb (red line), and 24.6% Sb (green line), respectively. The excitation power density was 1.6 W/cm^2 . (b) The OMR of InAs/InAsSb SLS with Sb composition of 26.3% at different excitation levels (black lines). The red lines show the theoretical response of the low-pass filter of the first order. The excitation power densities were 0.7, 0.9, 1.6 W/cm^2 . (c) The dependence of the PL response time constant on carrier excitation rate (Color figure online).

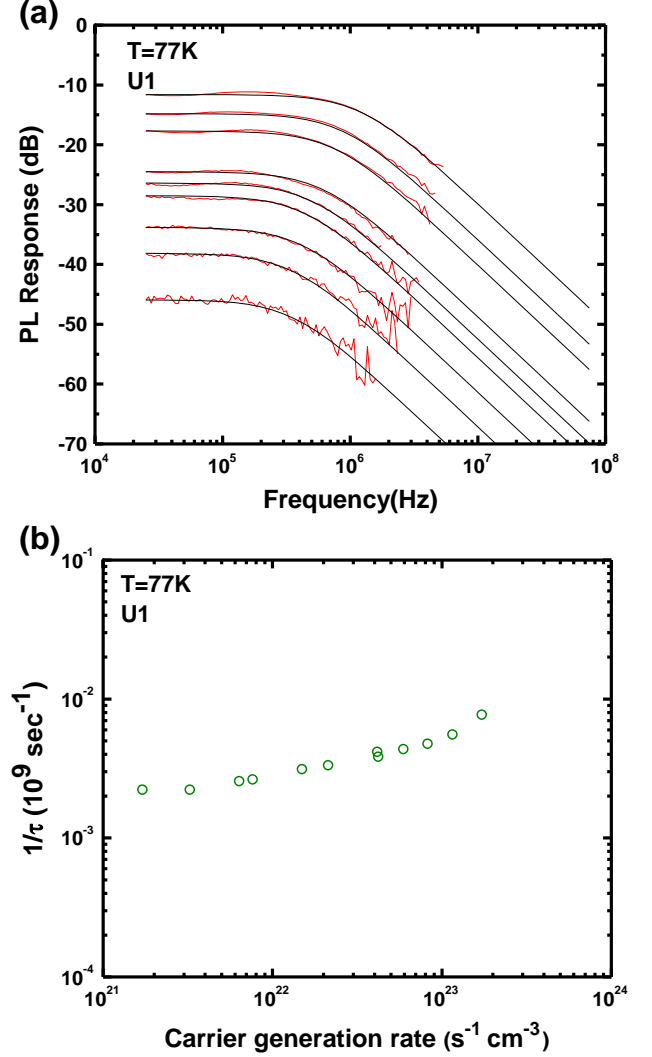


Fig. 5. (a) The OMR data for the Ga-free SLS with Sb composition of 23.5%, and without a AlSb barrier at different excitation levels (black lines). The red lines show the fit with the response of the first order low-pass filter. (b) The dependence of the PL response time constant on carrier excitation rate. The excitation power densities were 0.02, 0.04, 0.08, 0.09, 0.19, 0.27, 0.53, 0.54, 0.75, 1.05, 1.6, 2.2 W/cm^2 (Color figure online).

excitation power densities. It was concluded that the lowest power density was adequate for determining the minority carrier lifetime in P1, with excess concentration estimated to be $2.5 \times 10^{15} \text{ cm}^{-3}$.

For both samples, P1 and P2, the accuracy was within $\pm 1 \text{ ns}$ at the lowest power density used. For sample P1 with $\tau = 45 \text{ ns}$, this resulted in an accuracy of $\pm 2\%$, and for sample P2, with $\tau = 8 \text{ ns}$, the accuracy was estimated to be within $\pm 15\%$.

In contrast, for the undoped samples U1 and U2, this power level (1.6 W/cm^2) resulted in an underestimated lifetime of 200 ns. However, due to the longer lifetime and stronger PL intensity, the OMR data for undoped samples could be collected at two orders of magnitude lower excitation level (Figs. 5, 6). The lowest excess carrier concentration for the direct lifetime measurements was estimated to be

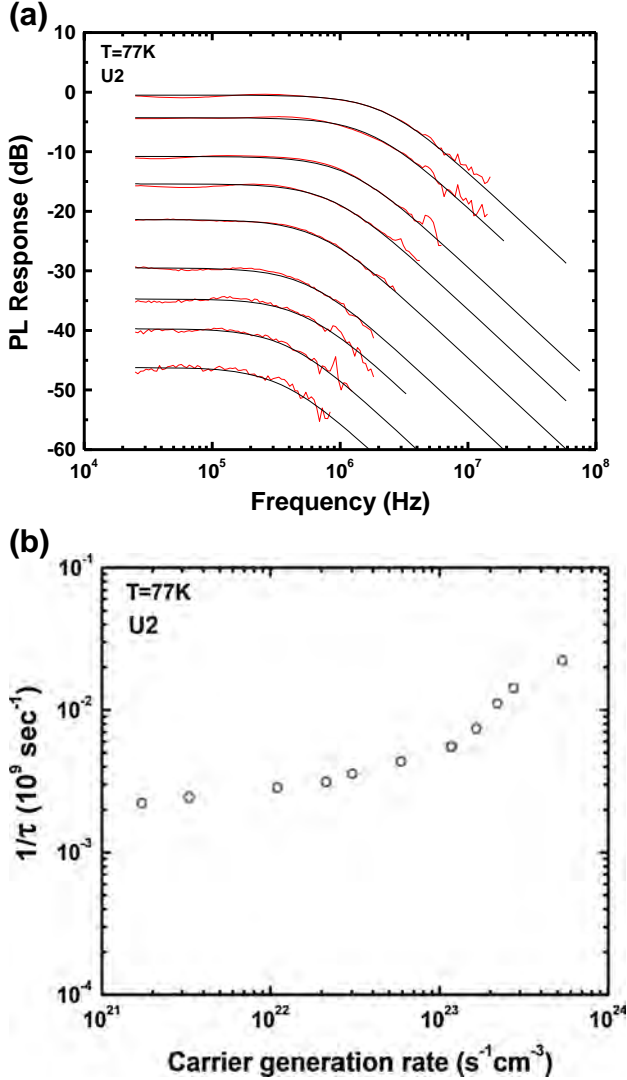


Fig. 6. (a) The OMR data for InAs/InAsSb SLs with Sb composition of 23.5%, with AlSb cap at different excitation levels (black lines). The red lines show the fit with the response of the first order low-pass filter. (b) The dependence of the PL response time constant on carrier excitation rate. The excitation power densities were 0.02, 0.04, 0.14, 0.27, 0.38, 0.75, 1.6, 2.2, 2.8, 3.5, 6.8 W/cm (Color figure online)².

$7 \times 10^{14} \text{ cm}^{-3}$. At this excitation level, the minority carrier lifetime in the undoped samples was found to be independent of excitation. The measurements resulted in the same lifetime constant of 450 ns at $T = 77 \text{ K}$ for both undoped samples.

SUMMARY

Electron lifetime values of 45 ns and 8 ns were measured at $T = 77 \text{ K}$ in Ga-free InAs/InAsSb SLS structures, p -doped to the levels of $6 \times 10^{16} \text{ cm}^{-3}$ and $3 \times 10^{17} \text{ cm}^{-3}$, respectively. Very good agreement was found between the target doping levels and the numbers derived from TRPL.

The product of the carrier lifetime and the carrier concentration at $T = 77 \text{ K}$ was found to be

nearly constant, which implies the minor role of Auger recombination in a InAs/InAsSb SLS with an energy gap of 0.165 eV and for hole concentrations up to the mid- 10^{17} cm^{-3} level. The decrease of the lifetime with doping is likely attributed to an increase of Be-derived SRH recombination centers, since the radiative lifetimes are expected to be much longer than the measured data.

In this work, we compare InAs/InAsSb and InAs/GaSb SLS structures with similar energy gaps (corresponding to wavelengths around $8 \mu\text{m}$) and similar electron lifetimes of 45 ns, and conclude that such lifetimes can be achieved at considerably higher doping concentrations for the Ga-free structure. Specifically, the same lifetime was achieved for doping levels of $6 \times 10^{16} \text{ cm}^{-3}$ in InAs/InAsSb SLS compared to the reported $1 \times 10^{16} \text{ cm}^{-3}$ doping level in the InAs/GaSb SLS. This suggests that photodetectors with p -doped InAs/InAsSb absorbers may exhibit lower dark currents due to a smaller diffusion component than those made with InAs/GaSb absorbers.

ACKNOWLEDGEMENTS

The work was supported by Army Research Office (Grants W911NF1110109 and W911NF1220057) and by National Science Foundation (Grant DMR1160843).

REFERENCES

1. G.A. Sai-Halasz, R. Tsu, and L. Esaki, *Appl. Phys. Lett.* 30, 651 (1977).
2. C.H. Grein, P.M. Young, M.E. Flatte, and H. Ehrenreich, *J. Appl. Phys.* 78, 15 (1995).
3. S. Bandara, P. Maloney, N. Baril, J. Pellegrino, and M. Tidrow, *Opt. Eng.* 50, 061015 (2011).
4. S. Bandara, N. Baril, P. Maloney, C. Billman, E. Nallon, T. Shih, J. Pellegrino, and M. Tidrow, *Infrared Phys. Technol.* 59, 18 (2013).
5. D. Hoffman, B.-M. Nguyen, P. Delaunay, A. Hood, M. Razeghi, and J. Pellegrino, *Appl. Phys. Lett.* 91, 143507 (2007).
6. B.C. Connelly, G.D. Metcalfe, H. Shen, and M. Wraback, *Appl. Phys. Lett.* 97, 251117 (2010).
7. D. Donetsky, G. Belenky, S.P. Svensson, and S. Suchalkin, *Appl. Phys. Lett.* 97, 052108 (2010).
8. D. Wang, D. Donetsky, S. Jung, and G. Belenky, *J. Electron. Mater.* 41, 3027 (2012).
9. W.G. Hu, Z. Wang, B.F. Su, Y.Q. Sai, S.J. Wang, and Y.W. Zhao, *Phys. Lett. A* 332, 286 (2004).
10. S.P. Svensson, D. Donetsky, D. Wang, H. Hier, F.J. Crowne, and G. Belenky, *J. Cryst. Growth* 334, 103 (2011).
11. G.C. Osbourn, *J. Vac. Sci. Technol. B* 2, 176 (1984).
12. D. Lackner, O.J. Pitts, M. Steger, A. Yang, M.L.W. Thewaltand, and S.P. Watkins, *Appl. Phys. Lett.* 95, 081906 (2009).
13. D. Lackner, O.J. Pitts, S. Najmi, P. Sandhua, K.L. Kavanagha, A. Yang, M. Steger, M.L.W. Thewalt, Y. Wang, D.W. McComb, C.R. Bolognesi, and S.P. Watkins, *J. Cryst. Growth* 311, 3563 (2009).
14. E.H. Steenbergen, Y. Huang, J.H. Ryou, R.D. Dupuis, K. Nunna, D.L. Huffaker, and Y.-H. Zhang, *AIP Conf. Proc.* 1416, 122 (2011).
15. E.H. Steenbergen, Y. Huang, J.-H. Ryou, L. Ouyang, J.-J. Li, D.J. Smith, R.D. Dupuis, and Y.-H. Zhang, *Appl. Phys. Lett.* 99, 071111 (2011).
16. D. Lackner, M. Steger, M.L.W. Thewalt, O.J. Pitts, Y.T. Cherng, S.P. Watkins, E. Plis, and S. Krishna, *J. Appl. Phys.* 111, 034507 (2012).

17. E.H. Steenberg, B.C. Connelly, G.D. Metcalfe, H. Shen, M. Wraback, D. Lubyshev, Y. Qiu, J.M. Fastenau, A.W.K. Liu, S. Elhamri, O.O. Cellek, and Y.-H. Zhang, *Appl. Phys. Lett.* 99, 251110 (2011).
18. B.V. Olson, E.A. Shaner, J.K. Kim, J.F. Klem, S.D. Hawkins, L.M. Murray, J.P. Prineas, M.E. Flatt, and T.F. Boggess, *Appl. Phys. Lett.* 101, 092109 (2012).
19. Y. Lin, D. Wang, D. Donetsky, L. Shterengas, G. Kipshidze, G. Belenky, S.P. Svensson, W.L. Sarney, and H.S. Hier, *J. Electron. Mater.* 42, 918 (2013).
20. H.S. Kim, O.O. Cellek, Zhi-Yuan Lin, Z.-Y. He, X.-H. Zhao, S. Liu, H. Li, and Y.-H. Zhang, *Appl. Phys. Lett.* 101, 161114 (2012).
21. D. Donetsky, S.P. Svensson, L.E. Vorobjev, and G. Belenky, *Appl. Phys. Lett.* 95, 212104 (2009).